Li *et al. Microstructures* **2025**, *5*, 2025036
DOI: 10.20517/microstructures.2024.84

Microstructures

Review

Open Access

Check for updates

Advances and advantages of metal-organic framework and its composite membrane as proton conduction materials

Long Li[1], Zhichao Shao[1], Weibing Liu[1], Kexin Gao[1], Yuanfeng Li[1], Haoran Cheng[1], Yi Wei[2], Xiutong Yu[1], Lei Su[1], Lipeng Zhai[1]

[1]Center for Advanced Materials Research, Zhongyuan University of Technology, Zhengzhou 450007, Henan, China.
[2]College of Chemistry, Zhengzhou University, Zhengzhou 450001, Henan, China.

Correspondence to: Prof. Zhichao Shao and Prof. Lipeng Zhai, Center for Advanced Materials Research, Zhongyuan University of Technology, 41 Zhongyuan Middle Road, Zhengzhou 450007, Henan, China. E-mail: shaozhichao@zut.edu.cn; zhailp@zut.edu.cn

How to cite this article: Li, L.; Shao, Z.; Liu, W.; Gao, K.; Li, Y.; Cheng, H.; Wei, Y.; Yu, X.; Su, L.; Zhai, L. Advances and advantages of metal-organic framework and its composite membrane as proton conduction materials. *Microstructures* **2025**, *5*, 2025036. https://dx.doi.org/10.20517/microstructures.2024.84

Received: 4 Sep2024 **First Decision:** 5 Dec 2024 **Revised:** 16 Dec 2024 **Accepted:** 25 Dec 2024 **Published:** 31 Mar 2025

Academic Editor: Zaiping Guo **Copy Editor:** Ping Zhang **Production Editor:** Ping Zhang

Abstract

The proton exchange membrane (PEM) fuel cell (FC) represents a new and efficient form of clean energy, offering unique advantages such as high power density and long service life. It is considered to be a promising new generation technology for addressing energy crises and environmental issues. However, the commercially available Nafion PEM continues to encounter issues such as insufficient water retention and elevated costs. It is imperative to develop PEM materials that exhibit high proton conductivity and superior stability. The optimal PEM material exhibits high proton conductivity, high chemical stability, superior mechanical properties, easy preparation, and low cost. These materials can be incorporated into H_2/O_2 fuel cells to enhance the practical application of metal-organic framework (MOF)-based proton-conductive materials in electrochemical devices. In recent years, MOFs have attracted considerable attention in the field of proton conduction owing to their tunable structure and high crystallinity. The incorporation of MOFs into polymer matrices has been shown to enhance the proton transfer path within the membrane, providing valuable insights into the mechanism of proton transfer in hybrid membranes. This review summarizes recent research on the advantages of using MOF materials for proton transfer and their composite membranes. It is crucial to develop PEM materials that exhibit high proton conductivity and outstanding stability.

Keywords: Metal-organic framework, composite membrane, proton conduction materials, PEMFC, proton exchange

INTRODUCTION

With the rapid growth of population and advancements in energy consumption technology, global energy consumption has reached an unprecedented level. To cope with increasing energy demand, we will have to double our current energy production (14 TW, 1TW = 1012 W) by 2050[1,2]. The main energy sources currently utilized are largely derived from fossil fuels, such as coal, petroleum, and natural gas, which together account for 80% of the global energy supply[3]. However, fossil energy reserves are gradually diminishing, and their combustion generates a wide array of toxic gases and volatile organic compounds, resulting in numerous environmental problems. A major concern is the global warming induced by the greenhouse effect, which has drawn significant attention. To address the energy crisis and the environmental challenges linked to the use of fossil fuels, it is crucial to explore cleaner alternative energy options, increase energy reserves and reduce the single dependence on fossil energy[4]. In this context, a number of alternative energy sources have been proposed, among which Fuel Cell (FC) technology is an attractive energy conversion system. The electrochemical reaction enables fuel cells to effectively transform the chemical energy from fuel into electrical energy, which is not bound by the Carnot cycle and provides high energy conversion efficiency[5]. In addition, fuel cells have a wide range of fuel sources (hydrogen, methanol, *etc.*), low environmental pollution, and a controllable assembly scale, making them a kind of clean energy with great application prospects[6-8]. Depending on the nature of the electrolyte, The FC can be divided into Alkaline FC (AFC), Phosphoric Acid FC (PAFC), Molten Carbonate FC (MCFC), Solid Oxide FC (SOFC), and Proton Exchange Membrane FC (PEMFC)[9-13]. PEMFCs are widely preferred by researchers because of their benefits, including low operating temperatures, quick start-up times, and the lack of electrolyte corrosion and leakage problems. These cells have seen significant advancements in recent decades.

PROTON EXCHANGE MEMBRANE FUEL CELLS

Introduction to PEMFC

The PEMFC is a fourth-generation fuel cell with superior power density and extended operational lifespan compared to other fuel cell types. At present, it has been extensively employed in compact portable power sources, meteorological observation stations and other fields, and can be used as a small power supply to meet the power supply needs of some specific places[14,15]. A PEMFC consists primarily of a cathode, an anode, and a proton exchange membrane (PEM) sandwiched in between [Figure 1][16]. The PEM serves as the electrolyte, while platinum/carbon acts as the catalyst. Hydrogen and methanol are used as fuels, with oxygen or air serving as the oxidant. Using hydrogen-oxygen fuel cells as an example, during operation, hydrogen gas is supplied to the anode, where it is catalyzed by the anode catalyst to break down into hydrogen ions and electrons. The hydrogen ions traverse the PEM to reach the cathode, while the electrons flow through the external circuit to the cathode, generating an electrical current. At the cathode, the hydrogen ions and electrons react with oxygen or air, which act as oxidizers, to form water molecules[17]. Specific responses are as follows:

Anode reaction:

$$H_2 = 2H^+ + 2e^- \quad (1)$$

Cathode reaction:

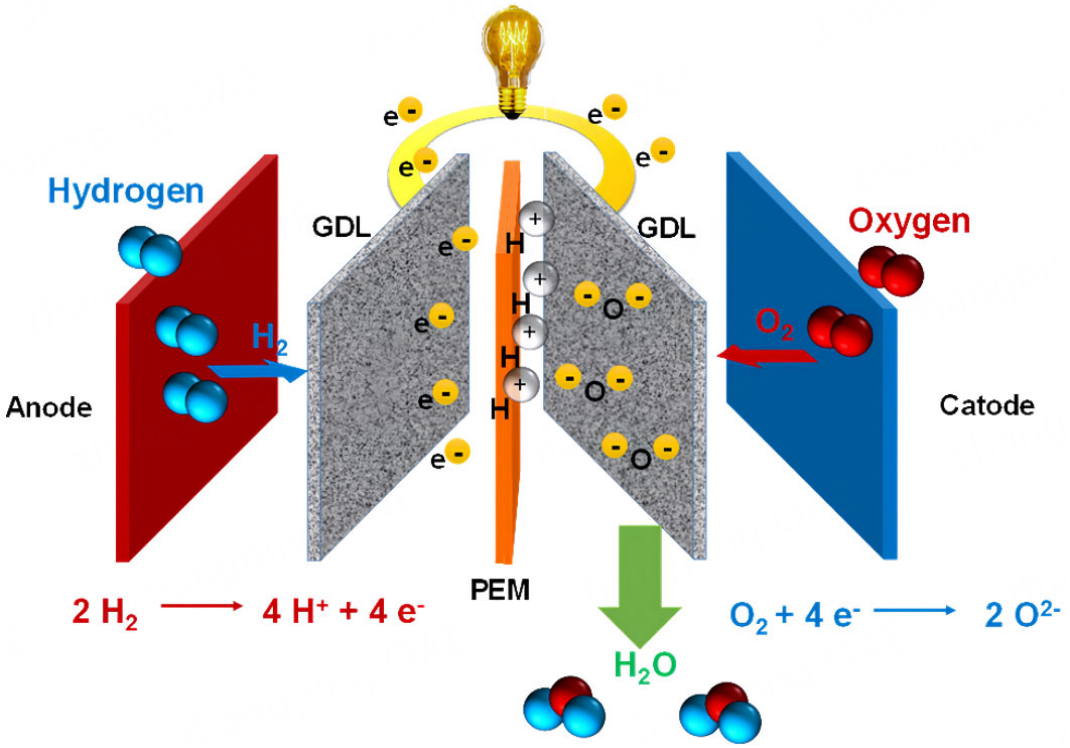

Figure 1. Working principle of PEMFC. (Reproduced with permission[16]. Copyright 2021, Multidisciplinary Digital Publishing Institute). PEMFC: Proton exchange membrane FC; FC: fuel cell.

$$2H^+ + \ O_2 + 2e^- = H_2O \tag{2}$$

Total response:

$$H_2 + \ O_2 = H_2O \tag{3}$$

As seen from the above equation, the product of the whole battery reaction is only water. The application and promotion of this battery will help achieve zero emissions of greenhouse and harmful gases, and mitigate the environmental issues arising from the utilization of fossil fuels.

Proton conduction mechanism

At present, there are two main explanations for proton conduction in PEMs. The first is the Grotthuss mechanism, which describes the transfer and diffusion of protons or proton defects through a hydrogen bond network formed by water molecules or other hydrogen bond carriers. Proposed by Theodore von Grotthuss in 1806, this mechanism involves hydrogen bond cleavage (cleavage energy of about 0.11 eV), resulting in an activation energy (E_a) generally between 0.1-0.4 eV[18]. The second explanation is the Vehicle mechanism [Figure 2], proposed by Ranjeesh *et al.* in 1982, where protons move with a proton carrier (H_2O, NH_3, *etc.*)[19]. In this case, the movement of the proton carrier demands a significant amount of energy, leading to an E_a for this transport mechanism that is typically greater than 0.4 eV. Consequently, proton mobility in the Vehicle mechanism is lower than in the Grotthuss mechanism because its diffusion process is much slower than the proton jump[20]. We evaluate the mechanisms of proton conduction by measuring the E_a, which is based on the differences between the two mechanisms.

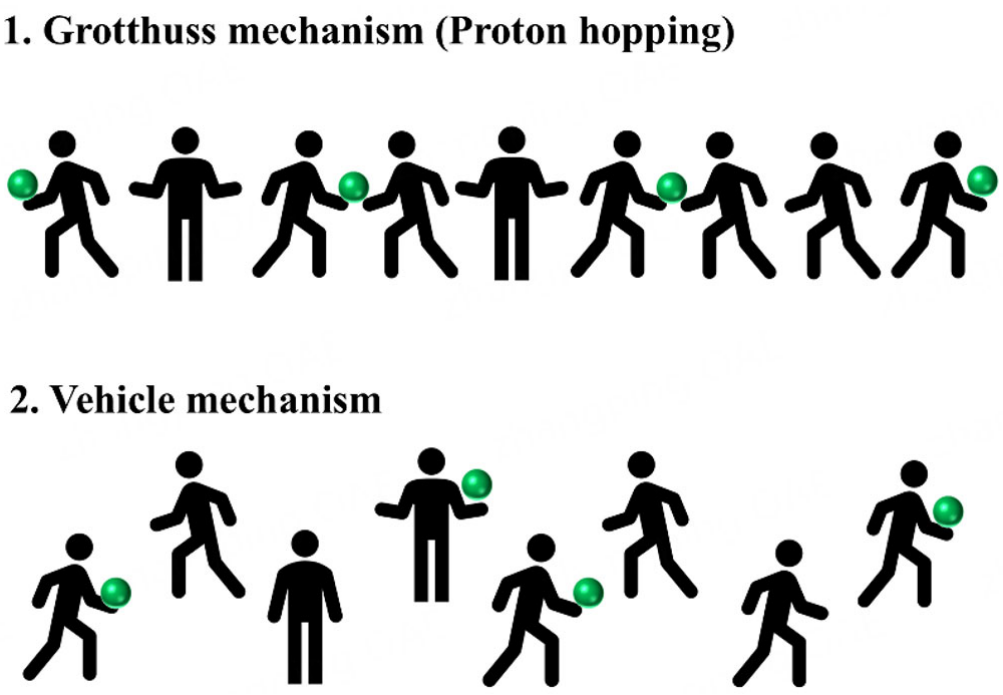

Figure 2. Proton conduction mechanism in proton exchange membrane.

Proton exchange membrane

The PEM is an essential element of the PEMFC, primarily functioning to isolate the anode from the cathode to prevent the direct interaction between the fuel and oxidant. It operates by blocking electron flow while enabling proton transport[6,21]. In order for PEMs to be utilized in fuel cells, they must meet the following performance requirements: High proton conductivity (σ) and the ability to block fuel; Appropriate water absorption and water retention capacity; Strong dimensional stability and chemical stability; A certain cost performance.

The Nafion membrane, developed by DuPont in the 1970s, is the most diffusely utilized PEM and is classified as one of the perfluorosulfonic acid membranes. In the hydrated state, a connected proton transport channel network can be formed inside the Nafion membrane, exhibiting excellent proton conduction ability (10^{-1}~10^{-2} S·cm^{-1}) and fuel cell output power during operation[22-24]. However, the formation of this channel depends heavily on the adsorption of the solvent (water). Therefore, when the working temperature is too high (above 80 °C), the weak water retention ability of Nafion membranes causes a large amount of absorbed water molecules to be lost, resulting in the interruption of some proton transport channels and a sharp decline in the film performance[25]. To address this limitation, researchers have developed several novel PEM materials.

Non-fluorinated sulfonated aromatic polymers, such as sulfonated polyether ether ketone (SPEEK), sulfonated polyimide (SPI), and sulfonated polyether sulfone (SPES), are considered as potential alternatives to Nafion membranes due to their exceptional mechanical properties, chemical stability, and high protonic conductivity[26-28]. Most of these polymers are obtained by sulfonation of highly stable aromatic compounds. Taking SPEEK as an example, Li *et al.* soaked polyether ether ketone (PEEK) in concentrated sulfuric acid to prepare a series of SPEEK films with different degrees of sulfonation[29]. The highly SPEEK showed excellent σ (80 °C, 10^{-2} S·cm^{-1}). However, with the increase of sulfonic acid groups, the mechanical and

chemical stability of SPEEK membranes deteriorates, which is also reflected in most other sulfonated aromatic polymers. Vinyl polymers such as polyvinyl alcohol (PVA) and polyethylpyrrolidone (PVP) are also used to prepare PEMs due to their strong hygroscopic properties, good σ and economic benefits[30-33]. However, due to their high solubility in water, it is difficult to work in high-humidity environments, and most of the current research focuses on low-humidity working conditions.

In addition to the above-mentioned PEMs, there are some fluorinated PEMs (BAM3G), chitosan (CS) and other PEMs, but they all face some defects and deficiencies in the practical application of fuel cells[34-36]. A single-component membrane material clearly fails to satisfy the requirements of a PEM; hence, the comprehensive properties of the polymer-based membrane need to be improved through techniques such as doping.

MOF MATRIX SUBCONDUCTOR AND ITS FUNCTIONALIZATION

Metal-organic frameworks (MOFs) are three-dimensional structures consisting of metal ions or clusters linked by organic ligands, resulting in a self-organized architecture[37]. The different metal nodes, ligands and connection modes lead to the diversification of the structure and function of MOFs. Through the design and adjustment of metal ions, ligands and reaction conditions, the structure and pore size of MOFs can be successfully adjusted, and then the properties of materials can be adjusted. Due to their advantages such as adjustable structure and high porosity, MOFs have been widely applied in various domains such as adsorption, sensing, catalysis, and luminescence, underscoring their essential significance in the field of materials science[38-43]. Moreover, they demonstrate significant potential for advancement in the area of proton conduction. On the one hand, due to their clear crystal structure and visual proton transport channel, MOFs are considered to be an ideal platform for a comprehensive understanding of proton conduction mechanisms[44]. On the other hand, the designability and adjustability of their structures and properties are also conducive to obtaining materials with high σ[45]. At present, functionalization of MOFs to enhance their intrinsic σ is mainly divided into two methods: modifying functional groups (-SO_3, -COOH, *etc.*) on the MOF skeleton and introducing guest molecules [Figure 3]. The creation of continuous hydrogen bonds within pores through ligand functionalization is essential for effective proton transfer. The addition of diverse functional groups can modify the surface and pore characteristics of MOFs. In particular, the inclusion of acidic functional groups increases the concentration of proton-conducting carriers in MOFs. Amines and hydroxyl groups, among other functional groups, can create additional proton hopping sites by establishing hydrogen bond networks. However, in the majority of rigid MOFs, the lack of water molecules or proton carriers frequently obstructs the formation of a continuous hydrogen bond network required for proton transfer at low humidity, resulting in a notable decrease in σ under these conditions. One of the primary characteristics of MOFs compared to other materials is their high porosity. This feature allows for the design and control of the pores and pore environment, which are critical advantages enabling their superior functionalities. Encapsulated guest molecules within the pores form hydrogen bonds with water molecules, facilitating the hopping of dissociated protons along these bonds. This process increases the carrier density and results in high diffusion efficiency. Consequently, the establishment of a continuous hydrogen bond network for proton transfer is essential in the design of proton-conducting MOFs. Although optimizing the pore environment and coordination mode can make the conductivity of electrolyte MOFs comparable to that of polymer proton-conducting materials such as Nafion, most current research on proton-conducting MOFs focuses on powders or single crystals, which significantly restricts their practical application in real fuel cell systems. Therefore, integrating MOF materials into the polymer matrix can enhance the hydrophilicity, acid-loading capacity, and mechanical strength of the polymer, while supplying abundant proton-conducting sites for the membrane materials. This method leads to a PEM with improved σ, thus expanding the practical applications of MOF-based PEMs.

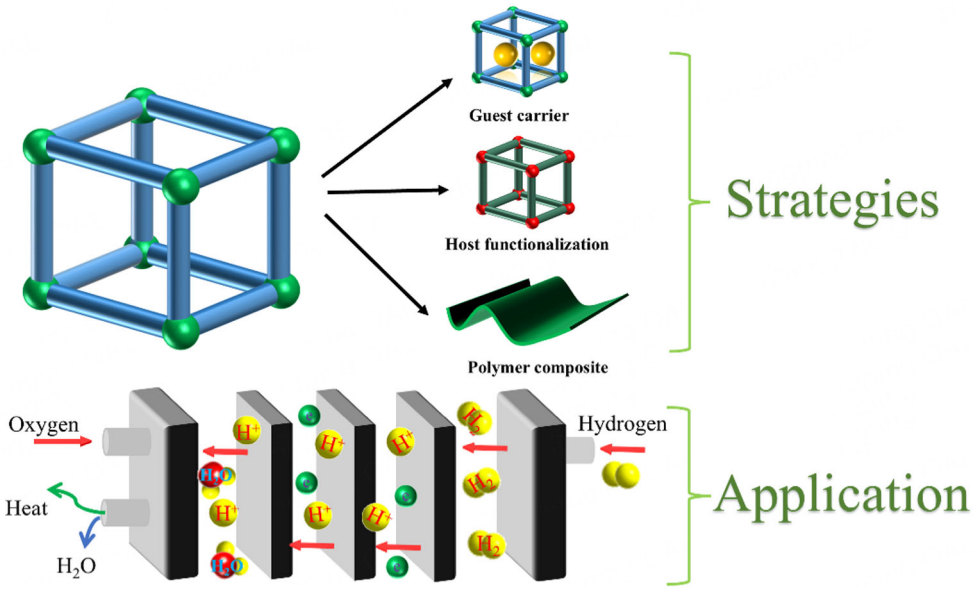

Figure 3. Development and application of proton transport materials based on MOFs. MOFs: Metal-organic frameworks.

Functionalized host framework increases the proton conductivity

In 2023, Xing *et al.* synthesized MOFs ($\{H[(N(CH_3)_4)_2][Gd_3(BDC\text{-}NO_2)_6]\}\cdot 3H_2O$) via hydrothermal synthesis[46], yielding a yellow prismatic crystal that incorporates the -NO_2 functional group. This material shows a high σ of 0.083 S/cm^{-1} at 65 °C and 95% relative humidity (RH), primarily because of the strong electron-withdrawing effect of the -NO_2 group, which significantly enhances proton dissociation from the carboxyl groups. Moreover, the coordination ability and hydrophilicity of the oxygen atoms in the carboxyl groups are substantially improved. Under photoinduction, BDC-NO_2 changes to BDC-NO. Density functional theory (DFT) calculations reveal that the electronegativity of the -NO group is relatively low, resulting in an increased hydrogen bond distance between BDC-NO and H_2O molecules. Consequently, this decreases the water adsorption energy for BDC-NO, impeding the formation of a stable hydrogen bond network and leading to a significant reduction in σ to 0.00046 S/cm^{-1} under the same experimental conditions [Figure 4A]. In 2024, Guo *et al.* successfully synthesized two types of MOFs with different functional groups: MOF-1 $\{[Zn_4(TIPE)_2(SO_4)_4(H_2O)]\cdot 5H_2O\}$, which contains sulfate groups, MOF-2 $\{[Zn_2(TIPE)(5\text{-}sip)(NO_3)_{0.66}]\cdot 0.34NO_3\cdot 17.5H_2O\}$[47], which contains sulfonic acid groups (where TIPE = 1,1,2,2-tetrakis(4-(1*H*-imidazole-1-yl)phenyl)-ethene and $H_3$5-sip=5-sulfoisophthalicacid). The influence of various functional groups on the σ of zinc-based MOFs was further investigated. The σ of both MOF-1 and MOF-2 were evaluated under a range of temperature and humidity conditions. At 90 °C with a RH of 98%, the maximum recorded σ for MOF-1 was found to be 4.48 × 10^{-3} S·cm^{-1}, whereas MOF-2 achieved a value of 5.69 × 10^{-2} S·cm^{-1} [Figure 4B]. In research conducted in 2022 by Ma *et al.*, they enhanced σ by grafting benzene-1,3,5-trisulfonic acid (BTSA) onto the Zr_6 cluster within PCN-222[48]. The substitution details of the PPCN-222-BTSA nanochannel and the changes in σ at different temperatures under completely wet conditions are shown in Figure 4C. It is evident that while the introduction of BTSA reduces pore volume, the resulting framework (PCN-222-BTSA) exhibits significant hydrophilicity. This modified structure demonstrates improved water absorption at lower RH levels and performs comparably to original PCN-222 at elevated humidity values. Due to enhanced water adsorption characteristics and the capacity of sulfonic groups to donate protons, PCN-222-BTSA displays a σ that exceeds pristine PCN-222 by two to three orders of magnitude. In another study from 2024, Yang *et al.* employed MOF-801 and UiO-66 as precursors to modify the pore architecture of composite MOFs[49]. As depicted in Figure 4D, utilizing MOF-

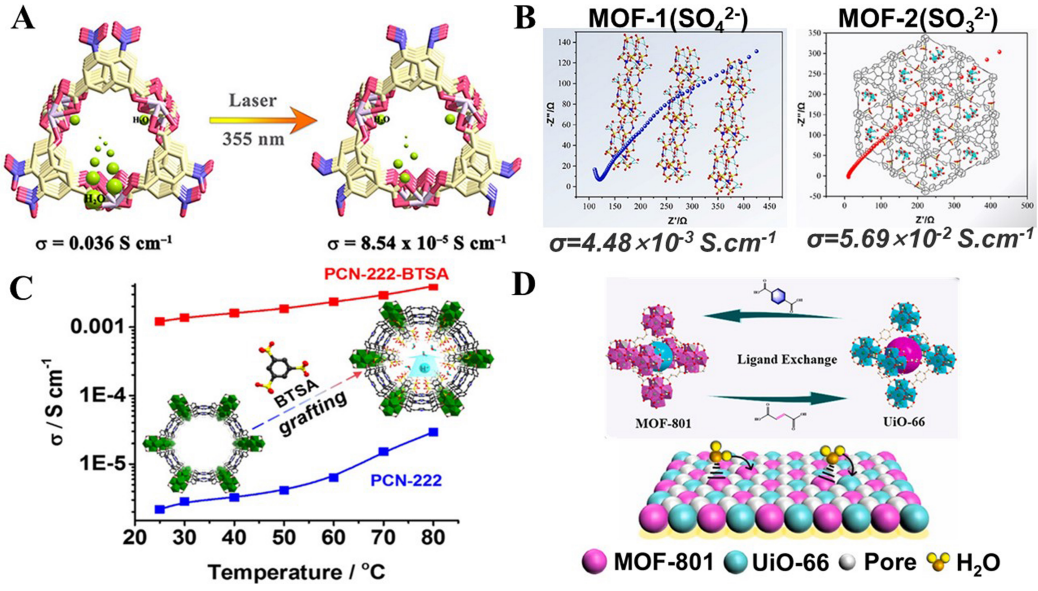

Figure 4. (A) The transformation of proton conductivity of Gd-NO_2 into Gd-NO under 355 nm photoinduction (Reproduced with permission[46]. Copyright 2023, Elsevier); (B) Effect of sulfate and sulfonate groups on the proton conductivity of Zn-based MOFs. (Reproduced with permission[47]. Copyright 2024, American Chemical Society); (C) Substitution description in PPCN-222-BTSA nanochannels and proton conductivity at 100% RH and different temperatures. (Reproduced with permission[48]. Copyright 2024, Elsevier); (D) Pore space and surface modification in pores improve proton conductivity of MOFs. (Reproduced with permission[49]. Copyright 2022, American Chemical Society). MOFs: Metal-organic frameworks; RH: relative humidity.

801 and UiO-66 as precursors, distinct MOF materials featuring varied pore structures were synthesized. By adjusting the molar ratio between fumaric acid and terephthalic acid, they optimized hydrogen bond networks and structural configurations which resulted in enhanced rates of proton transfer and increased material conductivity. A total of fourteen variants designated as MOF/MOG-801&UiO-66-X (where X denotes different molar ratios) were synthesized. Notably, MOG-801&UiO66-1:1 exhibited a measured σ value of 0.12 S·cm^{-1} at a temperature of 353 K under full humidity-five times greater than that observed for MOF-801&UIO-66-1:3 (which recorded 2.54 × 10^{-2} S·cm^{-1}), eleven times superior compared to the performance of pure MOF-801, and twenty-two times higher than UiO-66.

In 2024, Luo *et al.* introduced polymers containing sulfonic acid groups into the nanochannels of MOF compounds through *in-situ* synthesis[50]. It is widely acknowledged that high-concentration sulfonic acid nanomaterials have significant potential for use in proton conduction. They utilized (2)-acrylamido-2-methylpropane sulfonic acid (AMPS), a sulfonic acid-functionalized alkene, in combination with the crosslinking agent N,N'-methylenebisacrylamide (MBAA), to synthesize two MOF composites: PAMPS@MIL-101 and PAMPS@MIL-101-SO_3H. This synthesis was achieved through *in-situ* polymerization using free radical initiators within the highly stable MIL-101 structure. The integration of sulfonic acid polymers into the MOF channels exhibits strong adsorption capabilities for Ba^{2+} ions and ultra-high σ [Figure 5A]. At 85 °C and 95% RH, the two composite materials demonstrated remarkably high σ of 0.0643 S·cm^{-1} and 0.143 S·cm^{-1}, respectively. In 2024, Gao *et al.* established the CPM-200 system[51], comprising an In-ABTC-H_2O with a cationic [$In_3(\mu_3$-O)$(COO)_6$] cluster, a neutral [$InMn_2(\mu_3$-OH)$(COO)_6$]-based In/Mn-ABTC-H_2O, two anionic forms of [$Mn_3(\mu_3$-OH)$(COO)_6$]: Mn-ABTC-DMA, which features terminally coordinated N,N'-dimethylacetamide (DMA), and $Mn(H_2O)_6$@Mn-ABTC-H_2O, which incorporates H_3O^+ molecules. As shown in Figure 5B, the coordinated H_2O/H_3O^+ exhibits greater hydrophilicity than the DMA, resulting in enhanced acidity and absorption of more water molecules. When

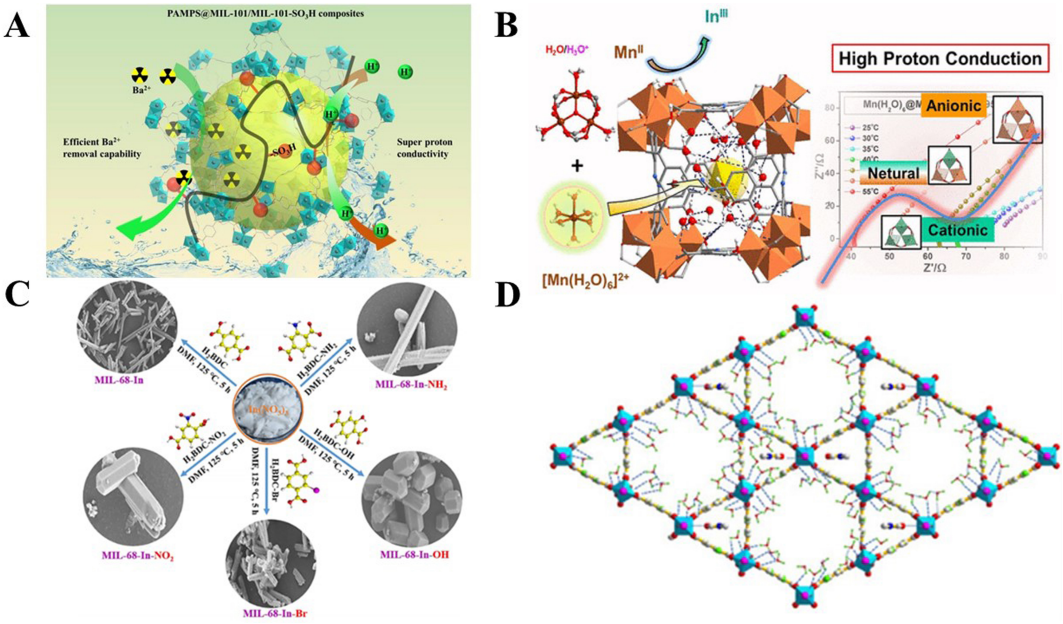

Figure 5. (A) The introduction of sulfonic acid polymer into the MOF channel shows strong adsorption capacity for Ba^{2+} and ultra-high proton conductivity. (Reproduced with permission[50]. Copyright 2024, Elsevier); (B) Custom porous ferrocene-based organic frame materials improve proton conductivity. (Reproduced with permission[51]. Copyright 2024, American Chemical Society); (C and D) Synthetic Process of the Five In-MOFs and the three-dimensional structure of MOF. (Reproduced with permission[52]. Copyright 2024, American Chemical Society). MOF: Metal-organic framework.

Mn(II) with the same oxidation state replaces In(III), the NO_3^- ions in In-ABTC-H_2O are concurrently substituted by the $[Mn(H_2O)_6]^{2+}$ cations in Mn-ABTC-H_2O, thus maintaining charge balance. Due to the combined effects of protonation at the metal nodes and a reduction in pore volume, the conductivity achieves 0.0115 S·cm^{-1}. However, under the same experimental conditions (328 K and 95% RH), the σ of In-ABTC-H_2O, In/Mn-ABTC-H2O, and Mn-ABTC-DMA are 0.0088 S·cm^{-1}, 0.0106 S·cm^{-1}, and 0.00231 S·cm^{-1}, respectively. In the same year, Song *et al.* used terephthalic acid (H_2BDC) or functionalized terephthalic acid (H_2BDC-X) as a multifunctional bond to efficiently prepare five three-dimensional isostructured In-MOFs of MIL-68-In or MIL-68-In-X (X = NH_2, OH, Br or NO_2) [Figure 5C and D][52]. Notably, their σ shows a significant positive correlation with temperature or RH and changes based on the functional groups on the organic ligand. Their maximum σ value is 10^{-3}-10^{-4} S·cm^{-1} (100 °C/98% RH), the sequence was MIL-68-In-OH (1.72 × 10^{-3} S·cm^{-1}) > Mil-68-In-NH_2 (1.70 × 10^{-3} S·cm^{-1}) > MIL-68-In-NO_2 (4.47 × 10^{-4} S·cm^{-1}) > MIL-68-In-Br (4.11 × 10^{-4} S·cm^{-1}) > MIL-68-In (2.37 × 10^{-4} S·cm^{-1}).

Introducing guest molecules to improve the proton conductivity of MOFs

MOFs possess a tunable pore structure and can be functionalized with a diverse range of molecules to enhance their performance. The introduction of functional molecules into the pores of MOFs has become a general strategy for high proton conductive materials. Comparison of σ and measurement conditions for MOFs-based proton conductors has been included in Table 1. In 2024, Wang *et al.* proposed a neutral frame ionization strategy to construct positive and negative charge centers to disperse and anchor encapsulated proton conducting molecules (PCMs) and modified MOF-867 with 1, 3-propanesultone (PS) to construct the N^+ and -SO_3^- sites of MOF-867 [Figure 6A][53]. Through electrostatic interactions, $CF_3SO_3^-$ and H^+ ions are effectively dispersed and anchored, resulting in the formation of a smooth proton transport channel that further enhances σ. MOF-867-PS-100TFOH exhibits a significantly improved σ exceeding 10^{-3} S·cm^{-1}), which is nearly two orders of magnitude greater than that of the original MOF-867 containing

Table 1. Comparison of proton conductivity and measurement conditions of MOF matrix subconductors

Compounds	σ S·cm^{-1}	RH (%)	T (°C)	Ref
MOF-867-PS-100TFOH	1.07 × 10^{-1} S·cm^{-1}	65	130	[53]
MOF-867-PS-100TFOH	2.79 × 10^{-1} S·cm^{-1}	33	130	[53]
MOF-867-PS-100TFOH	3.92 × 10^{-3} S·cm^{-1}	0	130	[53]
MOF-867-TFOH	3.71 × 10^{-4} S·cm^{-1}	0	130	[53]
MOF-867-PS-60TFOH	1.0 × 10^{-5} S·cm^{-1}	0	130	[53]
MOF-867-PS-100TFOH	1.06 × 10^{-3} S·cm^{-1}	0	30	[53]
MOF-867-PS-80TFOH	3.45 × 10^{-5} S·cm^{-1}	0	30	[53]
MOF-867@100TFOH	1.44 × 10^{-5} S·cm^{-1}	0	30	[53]
HKUST-1	4.83 × 10^{-5} S·cm^{-1}	75	80	[54]
LP-HKUST-1	1.53 × 10^{-4} S·cm^{-1}	75	80	[54]
MIM-CF_3SO_3@LP-HKUST-1-25%	4.77 × 10^{-2} S·cm^{-1}	75	80	[54]
MIM-CF_3SO_3@LP-HKUST-1-50%	5.61 × 10^{-2} S·cm^{-1}	75	80	[54]
MIM-CF_3SO_3@LP-HKUST-1-75%	7.46 × 10^{-2} S·cm^{-1}	75	80	[54]
MIM-CF_3SO_3@LP-HKUST-1-100%	3.41 × 10^{-1} S·cm^{-1}	75	80	[54]
MOF-801-Ce	2.59 × 10^{-3} S·cm^{-1}	98	100	[55]
Im@MOF-801-Ce	1.21 × 10^{-2} S·cm^{-1}	98	100	[55]
Hf-UiO-66-NO_2	3.41 × 10^{-1} S·cm^{-1}	98	100	[55]
Im@Hf-UiO-66-NO_2	8.94 × 10^{-4} S·cm^{-1}	98	100	[55]
NH_3@MOF-74(Co)	7.95 × 10^{-3} S·cm^{-1}	98	50	[56]

TFOH: CF_3SO_3H; PS: 1, 3-propanesultone; MOF-867-PS-XTFOH: where X is the volume of TFOH /μL per 100 mg of MOF; LP-HKUST-1: lager-pore HKUST-1; MIM-CF_3SO: N-methylimidazole triflate; RH: relative humidity; σ: proton conductivity; MOF: metal-organic framework.

isomolic acid, and it approaches the performance levels of leading anhydrophobic MOF composites [Figure 6B]. The composite of MOF-867-PS-XTFOH (where X is the volume of TFOH /μL per 100 mg of MOF) was obtained by adding CF_3SO_3H (TFOH). The plots of σ with temperature are presented in Figure 7A and B, and the analysis of the proton conduction mechanism of MOF-867-PS-XTFOH is shown in Figure 7C and D.

In the same year, Liu *et al.* incorporated varying proportions of N-methylimidazole trifluoride (MIM-CF_3SO_3) into HKUST-1 and lager-pore HKUST-1 (LP-HKUST-1)[54]. The resulting composites were designated as MIM-CF_3SO_3@HKUST-1-100% and MIM-CF_3SO_3@LP-HKUST-1-x (where x denotes 25%, 50%, 75%, and 100%). The σ of all materials was evaluated at a RH of 75% across a temperature range from 303 K to 353 K. The synthesis process for MIM-CF_3SO_3@LP-HKUST-1-x is shown in Figure 8A. The results show that the proportion of MIM-CF_3SO_3 in the LP-HKUST-1 hole is proportional to the σ of the material. Under these experimental conditions (at 353 K and 75% RH), the conductivity of each proton is (σ = 0.0477 S·cm^{-1}, σ = 0.0561 S·cm^{-1}, σ =0.0746 S·cm^{-1}.) MIM-CF_3SO_3@LP-HKUST-1-100% demonstrated exceptional σ (0.341 S·cm^{-1} at 353 K and 75% RH), representing an extraordinary increase by a factor of 7060 compared to HKUST-1, thereby positioning it among the highest values reported for MOFs in recent years [Figure 8B]. In 2023, Qiao *et al.* synthesized three-dimensional porous MOF (MOF-801-CE) with [$(NH_4)_2$Ce-$(NO_3)_6$] and fumaric acid as raw materials, and hot-synthesized Hf-UiO-66-NO_2 with $HfCl_4$ and 2-nitroterephthalic acid as raw materials [Figure 8C][55]. At 100 °C and 98% RH, the σ of MOF-801-Ce is 2.59 × 10^{-3} S·cm^{-1}, whereas that of Hf-UiO-66-NO_2 is 0.89 × 10^{-3} S·cm^{-1}. As shown in Figure 8D, imidazole molecules are incorporated into the pores of both MOFs via evaporation to further improve σ, leading to the formation of Im@MOF-801-Ce and Im@Hf-UiO-66-NO_2. The findings indicate that their σ values increase significantly by one order of magnitude to 10^{-2} S·cm^{-1}. In 2024, Wang *et al.* successfully encapsulated ammonia molecules into one-dimensional pores of MOF-74(Co) through ammonia vapor fumigation

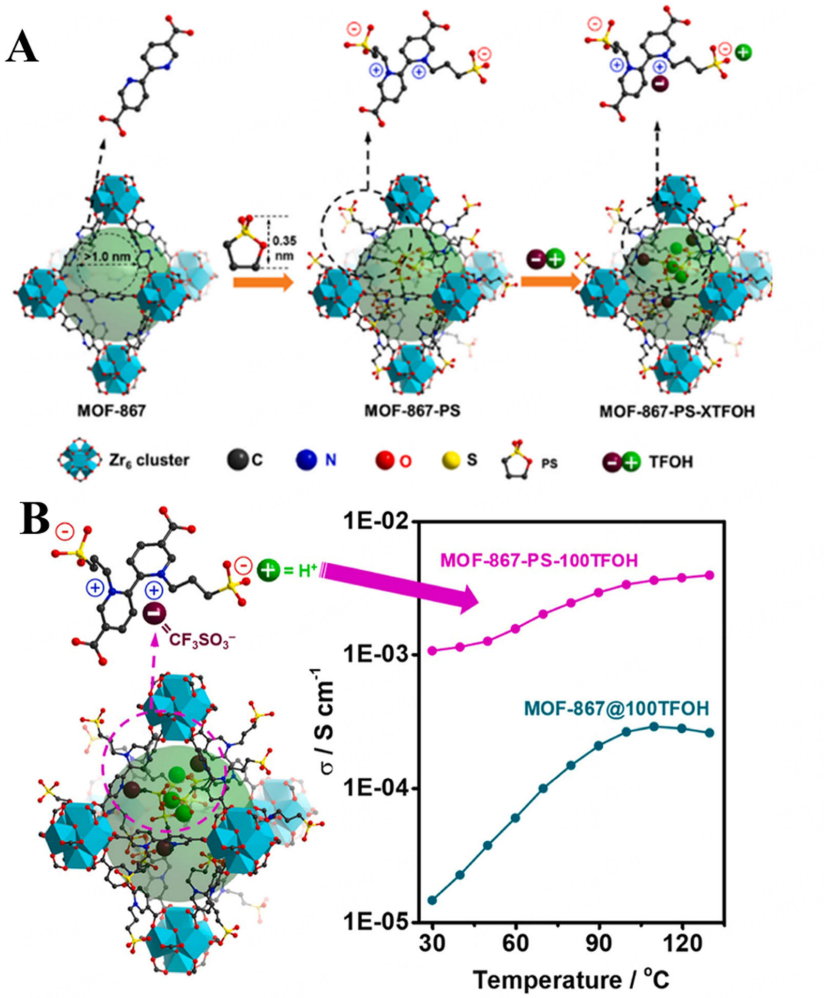

Figure 6. (A) Schematic ionization of MOF-867-PS and the dispersion and immobilization of the TFOH in MOF-867-PS-XTFOH; (B) Proton conductivity of MOF-867-PS-XTFOH and MOF-867-XTFOH at different temperatures. (Reproduced with permission[53]. Copyright 2024, Elsevier). MOF: Metal-organic framework.

[Figure 9A][56]. As illustrated in Figure 9B, Alternating current (AC) impedance measurements indicate that the σ of NH_3@MOF-74 (Co), which has been modified with ammonia, achieves a notable value of 6.8×10^{-3} $S \cdot cm^{-1}$. This marks a substantial improvement by a factor of 10,000 over the original MOF-74(Co) under conditions of 98% RH and 50 °C. The abundance and variety of hydrogen bonds in ammonia-modified compounds significantly enhance proton conduction.

COMPOSITE PROTON EXCHANGE MEMBRANE BASED ON MOFS

Although MOFs can achieve the same performance as Nafion and other polymer proton conductive materials by designing pores and the conductivity of coordination electrolytes, most studies on proton conductive MOF materials are based on powder or single crystal at present. The use of proton-conductive MOFs in actual fuel cells is considerably constrained by the difficulties in creating films from powdered and single-crystal rigid MOFs. In recent years, the benefits of MOF-organic polymer composite membranes, in conjunction with inorganic porous materials and the flexibility and ion-exchange properties of organic constituents, have provided a novel approach for the practical implementation of MOF-based PEMs. In 2024, Zhang *et al.* synthesized a bifunctional sulfamic acid UiO-66 (NUS) utilizing a one-pot solvothermal

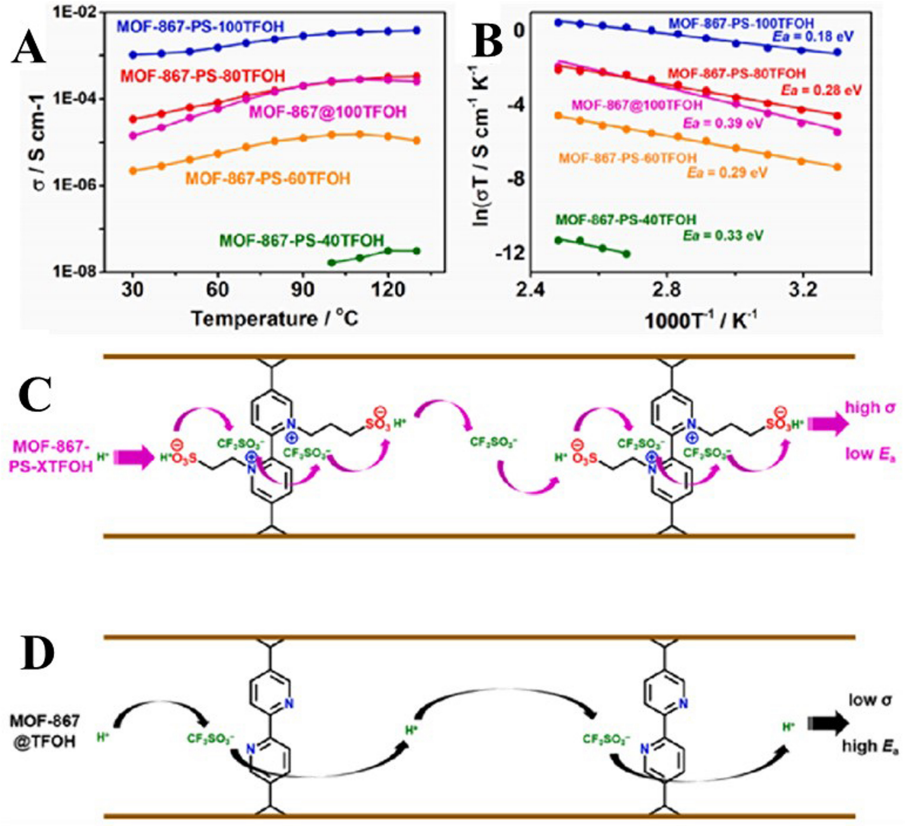

Figure 7. (A) Temperature-dependent proton conductivity; (B) Arrhenius plots; (C) the proposed proton hopping pathway in MOF-867-PS-XTFOH pores; (D) the proposed proton hopping pathway in MOF-867@100TFOH. (Reproduced with permission[53]. Copyright 2024, Elsevier). MOF: Metal-organic framework.

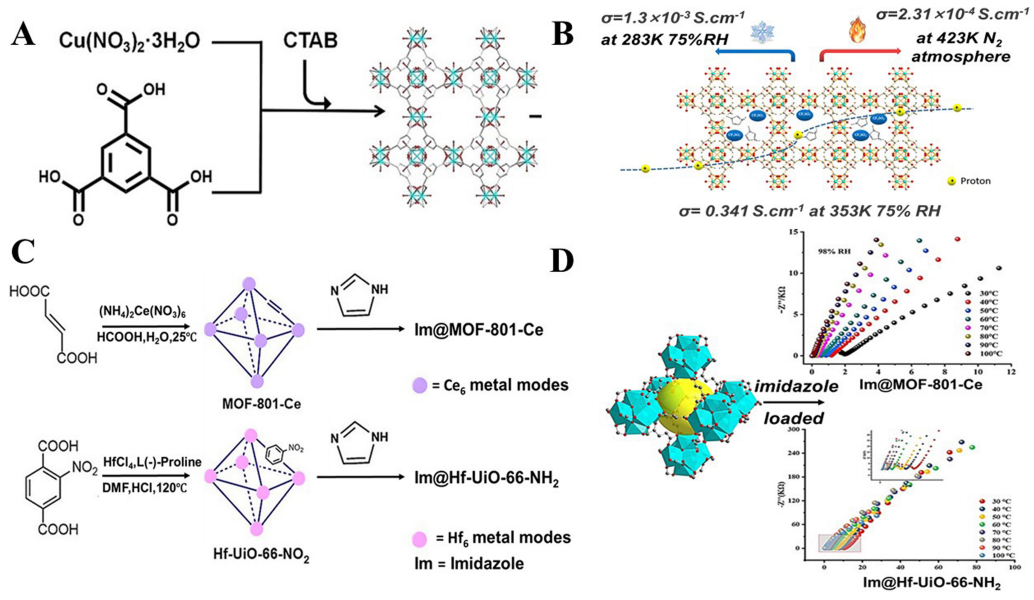

Figure 8. (A and B) Improving the proton conductivity of HKUST-1 by ionic liquid introduction. (Reproduced with permission[54]. Copyright 2024, Willey); (C and D) Imidazole-Anchored Strategy To Enhance the Proton Conductivity of Two Isostructural. (Reproduced with permission[55]. Copyright 2023, American Chemical Society).

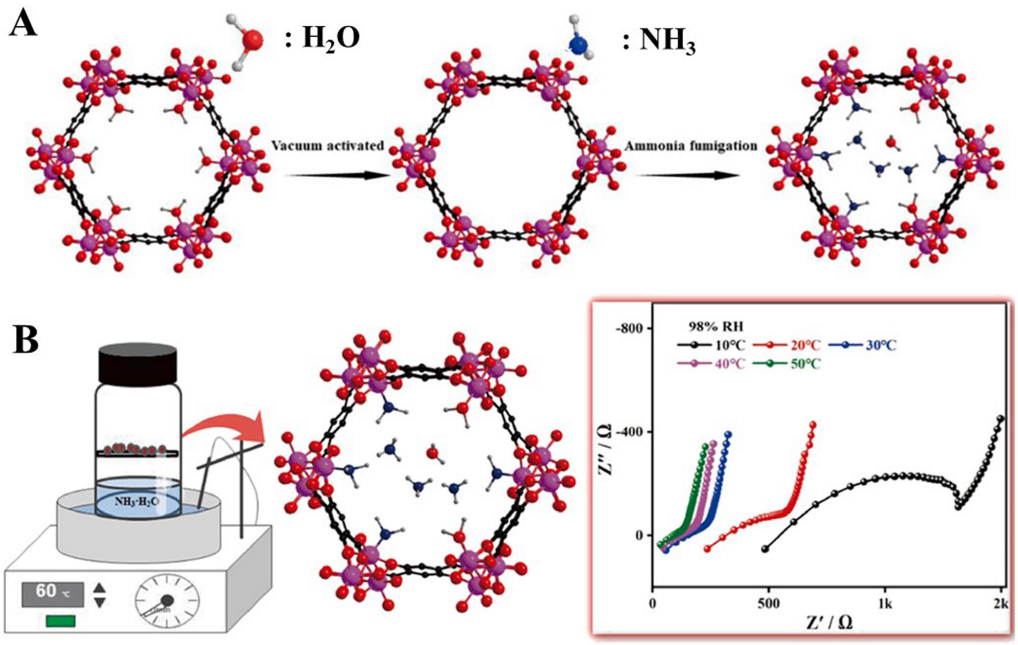

Figure 9. (A and B) Influence of encapsulating NH_3 molecules on proton conductivity of MOFs and a composite diagram of NH_3@MOF-74 (Co). (Reproduced with permission[56]. Copyright 2024, Elsevier). MOFs: Metal-organic frameworks.

method[57]. They combined NUS with an SPEEK matrix to fabricate hybrid films referred to as SPEEK/NUS-X (SPEEK/NUS-X) [Figure 10A]. Notably, SPEEK/NUS-1.5 exhibited a σ of 177.76 mS·cm^{-1} at 70 °C under conditions of 100% RH, maintaining stable performance over a period of 300 h. Its maximum power density reached 423.2 mW·cm^{-2}, approximately 2.20 times higher than that of the original SPEEK membrane. The proton conduction mechanism is shown in Figure 10B. Moreover, Long *et al.* present schematic diagrams detailing both the synthesis process for amino-pendant sulfonic acid bi-functionalized MOF material (UNCS) and the preparation methodology for SPEEK/UNCS-X composite membranes alongside [Figure 10C][58]. As shown in Figure 10D, the proton transport characteristics of the SPEEK/UNCS composite membrane are illustrated. The role played by UNCS remains consistent; it facilitates connections between proton donors and acceptors while minimizing E_a requirements to optimize long-distance conduction efficiency. In another study conducted in 2022 by Chen *et al.*, they incorporated a low degree of sulfonation (DS) into an SPEEK membrane using sulfamic acid bifunctional MOFs known as UNCS to enhance σ while preserving dimensional stability[59]. Figure 10E shows the movement pattern of protons within C-SPAEKS/IUSN-X2%. The single-cell performance of a PEM is positively correlated with its conductivity. Consequently, in addition to the pure C-SPAEKS membrane, we selected the membranes exhibiting the highest conductivity from two series of composite PEMs (C-SPAEKS/USN-4% and C-SPAEKS/IUSN-3%) as exemplars for evaluating single-cell performance, as illustrated in Figure 10F. The UNCS serves as a bridge between proton donors and acceptors, effectively reducing E_a barriers and shortening long-range conduction pathways for protons. At temperatures reaching up to 75 °C under full RH conditions, SPEEK/UNCS-3 achieved peak σ at an impressive value of 186.4 mS·cm^{-1}-significantly exceeding both original SPEEK and Nafion 117. These findings suggest the promising potential for the developed composite PEM to be applied in PEM fuel cells.

In a study conducted in 2022 by Ryu *et al.*, sulfonated polyethersulfone (sPSF) with a controllable DS was systematically synthesized[60]. The correlation between temperature and σ for Nafion 117, sPSF, and sPSF/sMOF (including sMIL-101 and sUiO-66) composite membranes at a concentration of 3 wt% was illustrated

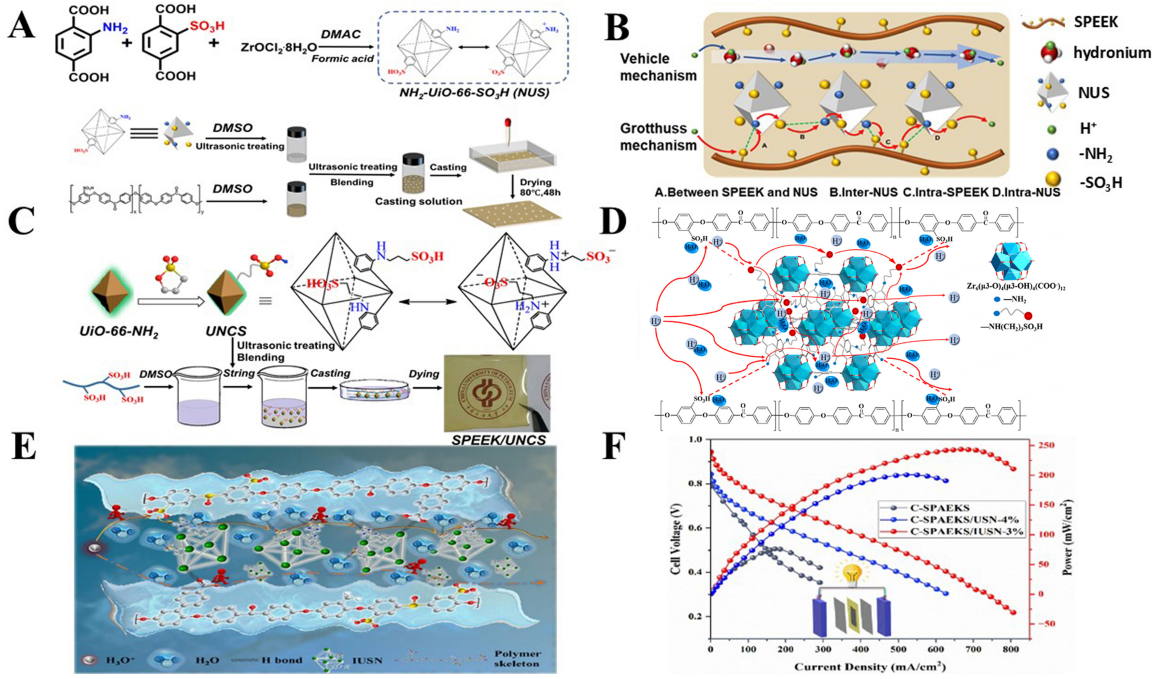

Figure 10. (A) Schematic illustration of preparation of (a) NUS, (b) SPEEK/NUS-X composite membranes; (B) Mechanism diagram of proton transport in SPEEK/NUS-X composite membranes. (Reproduced with permission[57]. Copyright 2024, Elsevier); (C) Schematic illustration of synthesis of UNCS and preparation of SPEEK/UNCS-X composite membranes. (Reproduced with permission[58]. Copyright 2022, Elsevier); (D) Schematic illustration of the proton transport of SPEEK/UNCS composite membranes. (Reproduced with permission[58]. Copyright 2022, Elsevier); (E) The proton movement mode in the C-SPAEKS/IUSN-X2% (Reproduced with permission[59]. Copyright 2022, Elsevier); (F) Single cell performance of C-SPAEKS, C-SPAEKS/USN-4% and C-SPAEKS/IUSN-3% at 80 °C, 100% RH. (Reproduced with permission[59]. Copyright 2022, Elsevier). RH: Relative humidity; SPEEK: sulfonated polyether ether ketone; NUS: amino-sulfonic acid bifunctionalized UiO-66; UNCS: an amino-pendant sulfonic acid bi-functionalized MOFs material; SPAEKS: sulfonated poly (aryl ether ketone sulfone)s.

in Figure 11A and B. Furthermore, they incorporated sulfonated MOFs (sMOFs; MIL-101(Cr)-SO_3H and UiO-66(Zr)-SO_3H) into the sPSF matrix to develop bissulfonated PSF/MOF composite films. With an optimal MOF loading of approximately ~3 wt%, these resulting sPSF/sMOF composite films demonstrated high σ (~0.18 S/cm) under fully humid ambient conditions. In another investigation in 2023 by Xing *et al.*, a SPES membrane incorporating a MOF was developed by integrating UiO-66-NH_2 into the primary aromatic polymer chain[61]. At 98% RH and 353 K, this composite membrane, which contains about 3% by mass of UiO-66-NH_2, exhibited a notable σ of 0.215 $S{\cdot}cm^{-1}$, a value 6.2 times higher than that commonly seen in traditional composite membranes. The proton transfer mechanism of the UiO-66-NH_2-SPES composite membrane and its σ under different experimental conditions are depicted in Figure 11C and D. These results highlight substantial progress in enhancing the σ of composite membranes and offer valuable insights for designing functional MOFs to improve performance in PEMs, along with effective methods for producing high-conductivity variants. In 2022, Ding *et al.* selected a rigid carboxylic acid ligand with nitro functional groups to coordinate with Tb(III) cations and successfully obtained TB-MOF with excellent macroporous hydrophilicity ({$[Tb_4(L)_4(OH)_4(H_2O)_3]{\cdot}8H_2O$}n, H_2L = 2-nitroterephthalic acid)[62]. The synthesis diagram and proton conduction diagram of Tb-MOF/Nafion-5 membrane were showed in Figure 11E and F. The synthesized Tb-MOF was integrated into a Nafion matrix to enhance its σ. At a Tb-MOF content of 5%, the composite membrane exhibited a σ of 1.53×10^{-2} $S{\cdot}cm^{-1}$ at 100% RH and 80 °C, which is approximately 1.81 times greater than that of pure Nafion membranes.

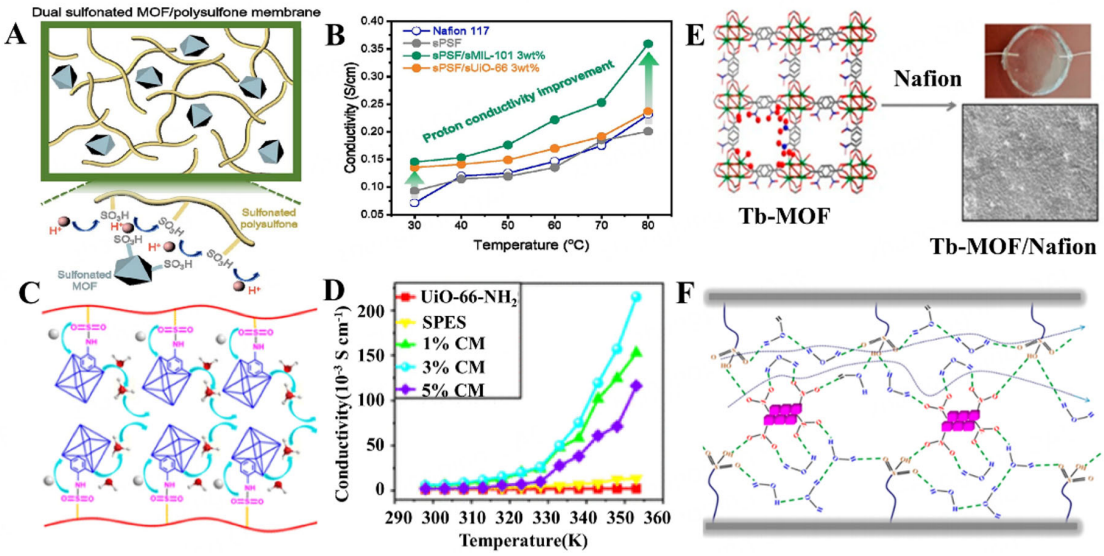

Figure 11. (A and B) Relationship between proton conductivity and temperature in Nafion 117, sPSF and sPSF/sMOF (sMIL-101 and sUiO-66) 3 wt% composite membranes. (Reproduced with permission[60]. Copyright 2022, Elsevier); (C and D) Proton transfer mechanism and proton conductivity of the UiO-66-NH_2-SPES composite membrane. (Reproduced with permission[61]. Copyright 2022, American Chemical Society); (E and F) Synthesis scheme and proton conduction diagram of Tb-MOF/Nafion-5 membrane. (Reproduced with permission[62]. Copyright 2022, American Chemical Society). MOF: Metal-organic framework; sPSF: sulfonated polyethersulfon.

In 2023, Chen *et al.* integrated HF-based MOFs into a CS matrix to fabricate a composite film exhibiting remarkable σ[63]. The proton transfer mechanism for the SA-1 and CBD-2 composite membranes and the synthesis process of this substance are illustrated in Figure 12A and 11B. Under optimal testing conditions, the measured σ of SA-1 and CBD-2 were determined to be 1.23 × 10^{-2} and 0.71 × 10^{-2} S·cm^{-1}, respectively. The CS/SA-1 and CS/CBD-2 composite films were synthesized using a casting technique. Experimental findings indicate that the incorporation of MOFs enhances both the stability and σ of the membrane, with peak σ values surpassing 10^{-2} S·cm^{-1} at temperatures reaching up to 100 °C under RH levels of 98%. In 2024, Liu *et al.* developed a composite material designated as MOF-808@MOG-808-X (where X denotes the mass ratio between MOF-808 and MOG-808) through grinding and blending methods[64], and the preparation of CS@MOF-808@MOG-808-1:2-Y was illustrated in Figure 12C. It was observed that the pore structure of MOF-808@MOG-808-1:2 is optimal, achieving maximum σ levels reaching up to 1.08 × 10^{-1} S·cm^{-1} at a temperature of 353 K with RH around 93%. This composite was subsequently blended with CS to produce composite PEMs, referred to as CS@MOF -808@MOG -808 -1:2-Y (with Y being either 5%,10% or 15%). Under similar experimental conditions, an impressive peak in σ was recorded-reaching an outstanding level of up to 1.19 × 10^{-2} S·cm^{-1} while maintaining stability. In 2024, Sun *et al.* employed polyvinylidene fluoride (PVDF) fibers as a substrate[65], which were subsequently modified with ethylenediamine to form an amine-functionalized crosslinked structure. Following this, UiO-66-NH_2 and UiO-66-NH_2-SO_3H were grown *in situ* on these fibers. The MOFs were then integrated with Nafion to fabricate nanofiber PEMs (NFPEMs) enhanced by MOF modification. Both UiO-66-NH_2 and UiO-66-NH_2-SO_3H were successfully incorporated into the system, leading to increases in σ of the MOF-supported films by 149.69% and 80.38%, respectively, compared to PVDF@Nafion. The successful incorporation of UiO-66-NH_2 and UiO-66-NH_2-SO_3H formed a new proton transport channel to further improve σ [Figure 12D]. Under conditions of 80 °C and 100% RH, the σ of the MOF-supported film reached an impressive value of 152.11 mS/cm.

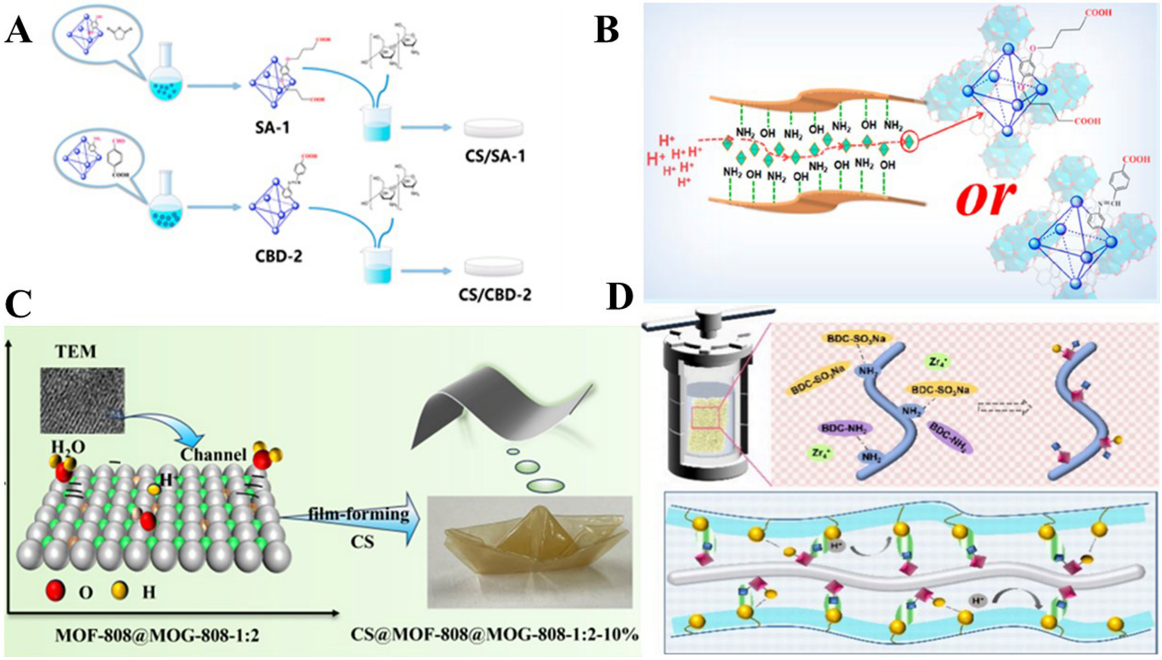

Figure 12. (A) Schematic illustration of preparation of CS/SA-1 and CS/CBD-2; (B) Proposed proton transfer mechanism of the SA-1 and CBD-2 composite membrane. (Reproduced with permission[63]. Copyright 2023, American Chemical Society); (C) The preparation of composite material improves the proton conductivity. (Reproduced with permission[64]. Copyright 2024, American Chemical Society); (D) The proton conductivity is further improved by establishing additional proton transport channels. (Reproduced with permission[65]. Copyright 2024, Elsevier).

In 2022, Bao *et al.* introduced Cu-MOF with acid-base excellent stability into polyvinylpyrrolidone/PVDF (PVP/PVDF, PP) in order to prepare hybrid films (Cu-MOF@PP-X, where X represents the percentage of Cu-MOF content)[66]. Nyquist diagram shows that due to the synergistic properties of the membrane, the σ is directly proportional to the content of Cu-MOF in the support matrix, and the σ of Cu-MOF@PP-50 is 2 orders of magnitude higher than that of the Cu-MOF sample under the same circumstances [Figure 13A]. The experimental findings show that the σ of Cu-MOF@PP-50 reaches 4.36×10^{-4} S·cm^{-1} at 353 K and 98% RH. This conductivity is roughly two orders of magnitude greater than that of pure Cu-MOF, demonstrating a conductivity of 1.91×10^{-6} S·cm^{-1}. In 2023, Yang *et al.* utilized the hollow polypyrrole (PPy) nanotube structure as a nitrogen source and successfully confined and separated cobalt nanoparticles on the surface of the PPy nanotube[67]. The fabrication process of PPy@ZIF-67 and the potential pathways for proton transfer and functional mechanisms within the PPy@ZIF-67/SPI membrane are illustrated [Figure 13B]. Ultimately, the imidazole-based zeolitic framework material ZIF-67 is anchored on the surface. Experimental findings indicate that the composite membrane displays superior ionic conductivity and power density, reaching 233.7 mS·cm^{-1} and 837 mW·cm^{-2} at 80 °C and 100% RH, respectively. The MOF architecture of the nanofibers offers multiple sites for proton hopping at the interface between the PPy@ZIF-67 filler and the matrix. Furthermore, the composite membrane efficiently supports proton transfer via both the Vehicle and Grotthuss mechanisms.

In addition to the above-mentioned reports on MOF-based PEMs, there are also some wonderful studies discussing the application of MOFs in practical PEMs and even fuel cells, which will not be repeated here. Despite this, progress in PEM design based on the performance of MOFs itself is still relatively slow. Currently, most MOF proton conductors are used to modify Nafion-dominated polymer electrolytes to enhance the conductivity and mechanical stability of PEMs, decrease their fuel permeability, and improve fuel cell performance. In addition, MOF materials enhanced proton conductance (10^{-2}~10^{-1} S·cm^{-1}) and

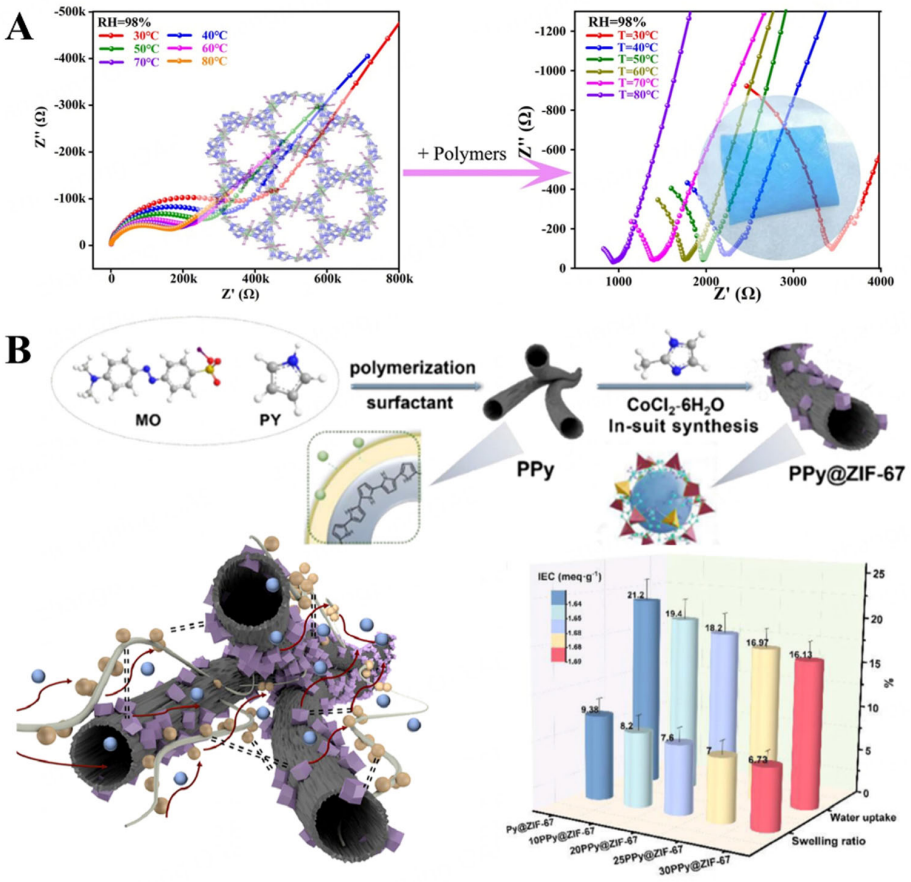

Figure 13. (A) The Nyquist plots for Cu-MOF and Cu-MOF@PP-50 at selected temperatures and 98% RH. (Reproduced with permission[66]. Copyright 2022, Elsevier); (B) Process description of the synthesis of PPy@ZIF-67 by *in-situ* growth method and Possible proton-transfer channel and functioning mechanism in PPy@ZIF-67/SPI film. (Reproduced with permission[67]. Copyright 2023, Elsevier). MOF: Metal-organic framework; RH: relative humidity; PPy: polypyrrole; SPI: sulfonated polyimide.

maintaining structural stability in the battery environment are not common, and there are only a dozen MOFs reaching the 10^{-1} S.cm^{-1} level so far. Therefore, the development of MOFs as real and effective PEM alternative materials is still facing great challenges.

SUMMARY AND OUTLOOK

Multifunctional MOFs with well-defined crystal structures and skeleton tunability demonstrate great application potential and unique preponderence in the field of proton conductors. A small change in the structure of an MOF has a huge effect on its σ. According to the structural characteristics of MOFs, the design strategy to obtain high σ mainly focuses on two aspects: increasing proton carrier concentration and constructing high-density hydrogen bond network[68]. The main sources of proton carriers are external guest molecules (water molecules, inorganic or organic acids, biological molecules, protonated organic molecules such as imidazole, histamine, *etc.*), countercations in the skeleton (H_3O^+, NH_4^+, $Me_2NH_2^+$, *etc.*), Lewis acidity of metal components and functionalized organic ligands (-SO_3H, -COOH, -OH, *etc.*). However, increasing the concentration of proton carriers usually reduces the crystallinity of MOFs or even destroys their skeleton integrity, so good stability is a prerequisite for the development of MOF proton conductors. On the other hand, the jump and diffusion of protons in pores often depend on hydrogen bond channels, and the effective and continuous hydrogen bond network between proton carriers and pores is the key to ensuring

the rapid transmission of protons.

In addition, the introduction of MOFs has a prodigious impact on the flexibility and mechanical properties of the composite films, and its high hardness particles often bring more defects to the composite membrane, making the membrane easy to break during use and weak long-term durability. In the future, we need to develop new techniques and design strategies, such as linear *in-situ* polymerization of MOF channels and ligands or self-assembly of small-size MOFs and polymers to enhance the quality and properties of composite films. Based on the design principle of proton conduction MOFs, on the premise of excellent hydrothermal stability, the synthesis of more MOF materials with enhanced proton conductance in a broad humidity scope and temperature range is a consistent goal for the development of new MOF electrolytes in years to come. The preparation of MOF composite PEMs with low cost, good mechanical properties and even repair functions, and their practical application in fuel cells are currently in the emerging stage, with great development potential, and need to be further developed by more researchers. It can be predicted that the development of porous material proton conductors will bring new developments to fuel cell technology.

DECLARATIONS

Authors' contributions

Made substantial contributions to conception and design of the study and performed data analysis and interpretation: Li, L.; Shao, Z.; Liu, W.; Gao, K.; Li, Y.; Cheng, H.; Wei, Y.; Yu, X.; Su, L.
Performed data acquisition and provided administrative, technical, and material support: Shao, Z.; Zhai, L.

Availability of data and materials

Not applicable.

Financial support and sponsorship

This work was financially supported by the Natural Science Foundation of Henan Province (232300421377), the Science and Technology Research and Development Program Joint Fund of Henan Province (232301420041), the Young Backbone Teacher Training Program of Henan Province (2023GGJS108) and China Postdoctoral Science Foundation (2022M722868).

Conflicts of interest

All authors declared that there are no conflicts of interest.

Ethical approval and consent to participate

Not applicable.

Consent for publication

Not applicable.

REFERENCES

1. Li, P.; Guo, M. Y.; Gao, L. L.; et al. Photoresponsivity and antibiotic sensing properties of an entangled tris(pyridinium)-based metal-organic framework. *Dalton. Trans.* **2020**, *49*, 7488-95. DOI
2. Dietl, C.; Hintz, H.; Rühle, B.; Schmedt, A. G. J.; Langhals, H.; Wuttke, S. Switch-on fluorescence of a perylene-dye-functionalized metal-organic framework through postsynthetic modification. *Chemistry* **2015**, *21*, 10714-20. DOI PubMed
3. Ye, Y.; Gong, L.; Xiang, S.; Zhang, Z.; Chen, B. Metal-organic frameworks as a versatile platform for proton conductors. *Adv. Mater.* **2020**, *32*, e1907090. DOI

4. Yuan, J.; Pan, Z.; Jin, Y.; et al. Membranes in non-aqueous redox flow battery: a review. *J. Power. Sources.* **2021**, *500*, 229983. DOI
5. Shao, Z.; Xue, X.; Gao, K.; et al. Sulfonated covalent organic framework packed Nafion membrane with high proton conductivity for H_2/O_2 fuel cell applications. *J. Mater. Chem. A.* **2023**, *11*, 3446-53. DOI
6. Chen, J.; Shao, Z.; Zhao, Y.; et al. Metal-ion coupling in metal-organic framework materials regulating the output performance of a triboelectric nanogenerator. *Inorg. Chem.* **2022**, *61*, 2490-8. DOI
7. Wen, T.; Shao, Z.; Wang, H.; Zhao, Y.; Cui, Y.; Hou, H. Enhancement of proton conductivity in fe-metal-organic frameworks by postsynthetic oxidation and high-performance hybrid membranes with low acidity. *Inorg. Chem.* **2021**, *60*, 18889-98. DOI
8. Yang, N.; Zhan, G.; Li, D.; Wang, X.; He, X.; Liu, H. Complete nitrogen removal and electricity production in thauera-dominated air-cathode single chambered microbial fuel cell. *Chem. Eng. J.* **2019**, *356*, 506-15. DOI
9. Chen, S.; Bocarsly, A.; Benziger, J. Nafion-layered sulfonated polysulfone fuel cell membranes. *J. Power. Sources.* **2005**, *152*, 27-33. DOI
10. Sajid, A.; Pervaiz, E.; Ali, H.; Noor, T.; Baig, M. M. A perspective on development of fuel cell materials: electrodes and electrolyte. *Intl. J. Energy. Res.* **2022**, *46*, 6953-88. DOI
11. Yang, Y.; Peltier, C. R.; Zeng, R.; et al. Electrocatalysis in alkaline media and alkaline membrane-based energy technologies. *Chem. Rev.* **2022**, *122*, 6117-321. DOI
12. Neergat, M.; Shukla, A. A high-performance phosphoric acid fuel cell. *J. Power. Sources.* **2001**, *102*, 317-21. DOI
13. Hu, L.; Lindbergh, G.; Lagergren, C. Performance and durability of the molten carbonate electrolysis cell and the reversible molten carbonate fuel cell. *J. Phys. Chem. C.* **2016**, *120*, 13427-33. DOI
14. Ma, R.; Gao, F.; Breaz, E.; Huangfu, Y.; Briois, P. Multidimensional reversible solid oxide fuel cell modeling for embedded applications. *IEEE. Trans. Energy. Convers.* **2018**, *33*, 692-701. DOI
15. Zhang, X.; Zhang, T.; Chen, H.; Cao, Y. A review of online electrochemical diagnostic methods of on-board proton exchange membrane fuel cells. *Appl. Energy.* **2021**, *286*, 116481. DOI
16. Tellez-Cruz, M. M.; Escorihuela, J.; Solorza-Feria, O.; Compañ, V. Proton exchange membrane fuel cells (PEMFCs): advances and challenges. *Polymers* **2021**, *13*, 3064. DOI PubMed PMC
17. Wang, H.; Wen, T.; Shao, Z.; et al. High proton conductivity in nafion/Ni-MOF composite membranes promoted by ligand exchange under ambient conditions. *Inorg. Chem.* **2021**, *60*, 10492-501. DOI
18. Shao, Y.; Yin, G.; Wang, Z.; Gao, Y. Proton exchange membrane fuel cell from low temperature to high temperature: material challenges. *J. Power. Sources.* **2007**, *167*, 235-42. DOI
19. Ranjeesh, K. C.; Illathvalappil, R.; Veer, S. D.; et al. Imidazole-linked crystalline two-dimensional polymer with ultrahigh proton-conductivity. *J. Am. Chem. Soc.* **2019**, *141*, 14950-4. DOI
20. Celis-Salazar, P. J.; Epley, C. C.; Ahrenholtz, S. R.; Maza, W. A.; Usov, P. M.; Morris, A. J. Proton-coupled electron transport in anthraquinone-based zirconium metal-organic frameworks. *Inorg. Chem.* **2017**, *56*, 13741-7. DOI PubMed
21. Laberty-Robert, C.; Vallé, K.; Pereira, F.; Sanchez, C. Design and properties of functional hybrid organic-inorganic membranes for fuel cells. *Chem. Soc. Rev.* **2011**, *40*, 961-1005. DOI PubMed
22. Shao, Z.; Huang, C.; Dang, J.; et al. Modulation of magnetic behavior and Hg^{2+} removal by solvent-assisted linker exchange based on a water-stable 3D MOF. *Chem. Mater.* **2018**, *30*, 7979-87. DOI
23. Paddison, S. Proton conduction mechanisms at low degrees of hydration in sulfonic acid-based polymer electrolyte membranes. *Annu. Rev. Mater. Res.* **2003**, *33*, 289-319. DOI
24. Mauritz, K. A.; Moore, R. B. State of understanding of nafion. *Chem. Rev.* **2004**, *104*, 4535-85. DOI PubMed
25. Xu, J.; Zhang, Z.; Yang, K.; Zhang, H.; Wang, Z. Synthesis and properties of novel cross-linked composite sulfonated poly (aryl ether ketone sulfone) containing multiple sulfonic side chains for high-performance proton exchange membranes. *Renew. Energy.* **2019**, *138*, 1104-13. DOI
26. Zhong, S.; Cui, X.; Cai, H.; Fu, T.; Zhao, C.; Na, H. Crosslinked sulfonated poly(ether ether ketone) proton exchange membranes for direct methanol fuel cell applications. *J. Power. Sources.* **2007**, *164*, 65-72. DOI
27. Yuan, Q.; Liu, P.; Baker, G. L. Sulfonated polyimide and PVDF based blend proton exchange membranes for fuel cell applications. *J. Mater. Chem. A.* **2015**, *3*, 3847-53. DOI
28. Muthumeenal, A.; Neelakandan, S.; Rana, D.; Matsuura, T.; Kanagaraj, P.; Nagendran, A. Sulfonated polyethersulfone (SPES) - charged surface modifying macromolecules (cSMMs) blends as a cation selective membrane for fuel cells. *Fuel. Cells.* **2014**, *14*, 853-61. DOI
29. Li, L.; Zhang, J.; Wang, Y. Sulfonated poly(ether ether ketone) membranes for direct methanol fuel cell. *J. Membr. Sci.* **2003**, *226*, 159-67. DOI
30. Wong, C. Y.; Wong, W. Y.; Loh, K. S.; et al. Development of poly(vinyl alcohol)-based polymers as proton exchange membranes and challenges in fuel cell application: a review. *Polym. Rev.* **2020**, *60*, 171-202. DOI
31. Bhowmick, G. D.; Dhar, D.; Ghangrekar, M. M.; Banerjee, R. TiO_2-Si- or $SrTiO_3$-Si-impregnated PVA-based low-cost proton exchange membranes for application in microbial fuel cell. *Ionics* **2020**, *26*, 6195-205. DOI
32. Guo, Z.; Xu, X.; Xiang, Y.; Lu, S.; Jiang, S. P. New anhydrous proton exchange membranes for high-temperature fuel cells based on PVDF-PVP blended polymers. *J. Mater. Chem. A.* **2015**, *3*, 148-55. DOI
33. Liang, X.; Zhang, F.; Feng, W.; et al. From metal-organic framework (MOF) to MOF-polymer composite membrane: enhancement of low-humidity proton conductivity. *Chem. Sci.* **2013**, *4*, 983-92. DOI

34. Basura, V.; Beattie, P.; Holdcroft, S. Solid-state electrochemical oxygen reduction at Pt|Nafion® 117 and Pt|BAM3G^{TM} 407 interfaces. *J. Electroanal. Chem.* **1998**, *458*, 1-5. DOI
35. Hu, F.; Zhong, F.; Wen, S.; et al. Preparation and properties of chitosan/organic-modified attapulgite composite proton exchange membranes for fuel cell applications. *Polym. Compos.* **2020**, *41*, 2254-62. DOI
36. Hu, F.; Li, T.; Zhong, F.; et al. Preparation and properties of chitosan/acidified attapulgite composite proton exchange membranes for fuel cell applications. *J. Appl. Polym. Sci.* **2020**, *137*, 49079. DOI
37. Kirchon, A.; Feng, L.; Drake, H. F.; Joseph, E. A.; Zhou, H. C. From fundamentals to applications: a toolbox for robust and multifunctional MOF materials. *Chem. Soc. Rev.* **2018**, *47*, 8611-38. DOI PubMed
38. Zhu, X.; Yang, C.; Yan, X. Metal-organic framework-801 for efficient removal of fluoride from water. *Microporous. Mesoporous. Mater.* **2018**, *259*, 163-70. DOI
39. Wang, R.; Xu, H.; Zhang, K.; Wei, S.; Deyong, W. High-quality Al@Fe-MOF prepared using Fe-MOF as a micro-reactor to improve adsorption performance for selenite. *J. Hazard. Mater.* **2019**, *364*, 272-80. DOI
40. Yassine, O.; Shekhah, O.; Assen, A. H.; Belmabkhout, Y.; Salama, K. N.; Eddaoudi, M. H_2S sensors: fumarate□based fcu□mof thin film grown on a capacitive interdigitated electrode. *Angew. Chem.* **2016**, *128*, 16111-5. DOI PubMed
41. Cao, Y.; Guo, X.; Wang, H. High sensitive luminescence metal-organic framework sensor for hydrogen sulfide in aqueous solution: A trial of novel turn-on mechanism. *Sensors. Actuators. B:. Chem.* **2017**, *243*, 8-13. DOI
42. Wang, C.; An, B.; Lin, W. Metal-organic frameworks in solid-gas phase catalysis. *ACS. Catal.* **2019**, *9*, 130-46. DOI
43. Lee, J.; Farha, O. K.; Roberts, J.; Scheidt, K. A.; Nguyen, S. T.; Hupp, J. T. Metal-organic framework materials as catalysts. *Chem. Soc. Rev.* **2009**, *38*, 1450-9. DOI PubMed
44. Sadakiyo, M.; Yamada, T.; Kitagawa, H. Hydrated proton-conductive metal-organic frameworks. *Chempluschem* **2016**, *81*, 691-701. DOI PubMed
45. Li, X.; Wang, Y.; Wu, B.; Zeng, L. Efficient proton transport in stable functionalized channels of zirconium metal-organic frameworks. *ACS. Appl. Energy. Mater.* **2021**, *4*, 8303-10. DOI
46. Xing, X. S.; Zhou, Z.; Gao, Q.; et al. Photomodulation of proton conductivity by nitro-nitroso transformation in a metal-organic framework. *Inorg. Chem.* **2023**, *62*, 18809-13. DOI
47. Guo, Y. Y.; Wang, R. D.; Wei, W. M.; et al. Comparative analysis of proton conductivity in two Zn-based MOFs featuring sulfate and sulfonate functional groups. *Inorg. Chem.* **2024**, *63*, 3870-81. DOI
48. Ma, Y.; Liu, J.; Yan, W.; et al. Improving the proton conductivity of MOF materials by regulating the pore space. *Microporous. Mesoporous. Mater.* **2024**, *367*, 112974. DOI
49. Yang, F.; Shi, R.; Huang, H.; et al. Nanochannel engineering in metal-organic frameworks by grafting sulfonic groups for boosting proton conductivity. *ACS. Appl. Energy. Mater.* **2022**, *5*, 3235-41. DOI
50. Luo, G.; Jiang, J.; Wei, S.; et al. Introducing sulfonic acid polymers into MOF nanochannels for ultra-high Ba^{2+} adsorption capacity and proton conductivity. *Sep. Purif. Technol.* **2024**, *343*, 127133. DOI
51. Gao, H.; Yu, L.; Zhang, J.; Gao, J.; Zhang, X. High proton conduction for CPM-200 achieved by aliovalent-predefinition of $M_3(\mu_3\text{-O})$ building blocks and in situ encapsulation of hydrated metal ions. *ACS. Materials. Lett.* **2024**, *6*, 765-71. DOI
52. Song, Y. J.; Sang, Y. L.; Xu, K. Y.; Hu, H. L.; Zhu, Q. Q.; Li, G. Ligand-functionalized MIL-68-type indium(III) metal-organic frameworks with prominent intrinsic proton conductivity. *Inorg. Chem.* **2024**, *63*, 4233-48. DOI PubMed
53. Wang, K.; Si, L.; Tian, Y.; Yang, F.; et al. Ionization of a neutral MOF to disperse and anchor acid for boosting anhydrous proton conductivity. *Microporous. Mesoporous. Mater.* **2024**, *363*, 112825. DOI
54. Liu, Y.; Liu, Y.; Zheng, X.; et al. Improving the proton conductivity of HKUST-1 by hole expansion and ionic liquid introduction. *Appl. Organomet. Chem.* **2024**, *38*, e7383. DOI
55. Qiao, J. Q.; Ren, H. M.; Chen, X.; Li, Z. F.; Li, G. Icing on the cake: imidazole-anchored strategy to enhance the proton conductivity of two isostructural Ce(IV)/Hf(IV) metal-organic frameworks. *Inorg. Chem.* **2023**, *62*, 21309-21. DOI
56. Wang, Q.; Jiang, F.; Zhang, R.; et al. Enhancing proton conduction of MOF-74(Co) by encapsulating NH_3 molecules. *J. Solid. State. Chem.* **2024**, *335*, 124696. DOI
57. Zhang, X.; Long, J.; Wang, M.; Liu, Y.; Ma, H. Using bifunctionalized NH_2-UiO-66-SO_3H to improve the performance of sulfonated poly (ether ether ketone) in proton exchange membranes. *Int. J. Hydrogen. Energy.* **2024**, *61*, 1495-504. DOI
58. Long, J.; Zhang, X.; Zeng, S.; et al. Constructing a long-range proton conduction bridge in sulfonated polyetheretherketone membranes with low DS by incorporating acid-base bi-functionalized metal organic frameworks. *Int. J. Hydrogen. Energy.* **2023**, *48*, 2001-12. DOI
59. Chen, X.; Ren, Q.; Xu, J.; Ju, M.; Meng, L.; Wang, Z. Design, transport efficiency and structure-activity relationship of sulfonated poly (aryl ether ketone) proton exchange membrane based on multi-functional MOFs. *Electrochim. Acta.* **2023**, *469*, 143210. DOI
60. Ryu, G. Y.; An, S. J.; Yu, S.; et al. Dual-sulfonated MOF/polysulfone composite membranes boosting performance for proton exchange membrane fuel cells. *Eur. Polym. J.* **2022**, *180*, 111601. DOI
61. Xing, Y. Y.; Wang, J.; Zhang, C. X.; Wang, Q. L. High proton conductivity of the UiO-66-NH_2-SPES composite membrane prepared by covalent cross-linking. *ACS. Appl. Mater. Interfaces.* **2023**, *15*, 33003-12. DOI
62. Ding, L.; Zou, H.; Lu, J.; et al. Enhancing proton conductivity of nafion membrane by incorporating porous tb-metal-organic framework modified with nitro groups. *Inorg. Chem.* **2022**, *61*, 16185-96. DOI
63. Chen, X.; Zhang, S. L.; Xiao, S. H.; Li, Z. F.; Li, G. Ultrahigh proton conductivities of postmodified Hf(IV) metal-organic frameworks

and related chitosan-based composite membranes. *ACS. Appl. Mater. Interfaces.* **2023**, *15*, 35128-39. DOI

64. Liu, J.; Yan, W.; Ma, Y.; et al. Improving proton-conducting stability by regulating pore size of MOF materials through mixed grinding. *ACS. Appl. Mater. Interfaces.* **2024**, *16*, 34240-53. DOI
65. Sun, J.; Han, D.; Dong, R.; et al. Enhancing proton conductivity and dimensional stability of nanofiber proton exchange membranes through in situ growth of MOF-Modified PVDF nanofibers. *Energy. Fuels.* **2024**, *38*, 7322-30. DOI
66. Bao, Y.; Zheng, J.; Zheng, H.; et al. Cu-MOF@PVP/PVDF hybrid composites as tunable proton-conducting materials. *J. Solid. State. Chem.* **2022**, *310*, 123070. DOI
67. Yang, J.; Lin, J.; Sun, S.; Li, X.; Liu, L.; Wang, C. Multidimensional network of polypyrrole nanotubes loaded with ZIF-67 to construct multiple proton transport channels in composite proton exchange membranes for fuel cells. *J. Mater. Sci. Technol.* **2023**, *152*, 75-85. DOI
68. Shi, Y.; Wu, M.; Ge, S.; et al. Advanced functional electromagnetic shielding materials: a review based on micro-nano structure interface control of biomass cell walls. *Nanomicro. Lett.* **2024**, *17*, 3. DOI PubMed PMC